Article

NMR Structural Study of the Prototropic Equilibrium in Solution of Schiff Bases as Model Compounds

David Ortegón-Reyna [1], Cesar Garcías-Morales [2], Itzia Padilla-Martínez [3], Efren García-Báez [3], Armando Aríza-Castolo [2], Ana Peraza-Campos [1] and Francisco Martínez-Martínez [1,*

[1] Laboratorio de Posgrado, Facultad de Ciencias Químicas, Universidad de Colima, Km 9 Carretera Colima-Coquimatlán, Colima 28400, Mexico; E-Mails: dortegon@ucol.mx (D.O.-R.); peraza@ucol.mx (A.P.-C.)

[2] Departamento de Química, Centro de Investigación y Estudios Avanzados del Instituto Politécnico Nacional, Av. IPN 2508, San Pedro Zacatenco 07360, México D. F., Mexico; E-Mails: cgarciam@cinvestav.mx (C.G.-M.); aariza@cinvestav.mx (A.A.-C.)

[3] Departamento de Ciencias Básicas, Unidad Profesional Interdisciplinaria de Biotecnología del Instituto Politécnico Nacional, Av. Acueducto s/n Barrio la Laguna Ticomán, México D. F. 07340, Mexico; E-Mails: ipadillamar@ipn.mx (I.P.-M.); efren1003@yahoo.com.mx (E.G.-B.)

__*__ Author to whom correspondence should be addressed; E-Mail: fjmartin@ucol.mx; Tel./Fax: +52-312-316-1163.

Abstract: An NMR titration method has been used to simultaneously measure the acid dissociation constant (pK_a) and the intramolecular NHO prototropic constant ΔK_{NHO} on a set of Schiff bases. The model compounds were synthesized from benzylamine and substituted *ortho*-hydroxyaldehydes, appropriately substituted with electron-donating and electron-withdrawing groups to modulate the acidity of the intramolecular NHO hydrogen bond. The structure in solution was established by ^{1}H-, ^{13}C- and ^{15}N-NMR spectroscopy. The physicochemical parameters of the intramolecular NHO hydrogen bond (pK_a, ΔK_{NHO} and $\Delta\Delta G°$) were obtained from ^{1}H-NMR titration data and pH measurements. The Henderson–Hasselbalch data analysis indicated that the systems are weakly acidic, and the predominant NHO equilibrium was established using Polster–Lachmann δ-diagram analysis and Perrin model data linearization.

Keywords: Schiff bases; NHO prototropic tautomerism; NMR titration; δ-diagram

1. Introduction

Schiff bases are a great topic of basic research, that to date have an important place in organic chemistry and they have a great versatility in different fields of study. They have different biologic applications as antitumor agents [1–5], in the strengthening of immune response for cancer, in leukemia, in HIV, as anticonvulsant, antibacterials, antifungal, antiinflammatory, as prodrugs [6–15] and as study models in the intramolecular hydrogen bond from cofactor pyridoxal-5-phosphate [16–20]. They are also of interest because of their solvatochromic, thermochromic and photochromic properties with applications in optical recording technology, molecular electronics and photonics [21–30].

The Schiff bases derived from *ortho*-hydroxyaromatic aldehydes that are pentaconjugated non-symmetric systems [31] in which proton transfer from the oxygen hydroxyl to the nitrogen of imine, through the NHO hydrogen bond is observed (Scheme 1) have been extensively studied in recent years [32–46].

Scheme 1. Prototropic 1,5 rearrangement in Schiff bases.
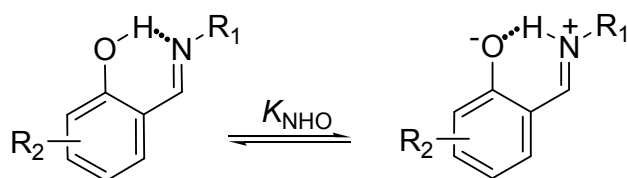
In these investigations several analytical methods for determining the prototropic equilibrium have been applied, such as FT-IR spectroscopy and X-ray diffraction in the solid state [45–48], as well as solution ^{1}H-, ^{13}C- and ^{15}N-NMR [33,34,49–51]. This 1,5 tautomeric equilibrium is directly affected by the substituents [52–56] attached to both the phenyl group and the imine nitrogen which exert a strong influence on the acidity of the OH group, the basicity of the nitrogen atom and thus the NHO bond strength. Substituents also greatly increase the stability of the compounds by the effect of hydrogen bonding assisted by resonance (RAHB) [57–59]; preferences have been found in the position of the hydrogen either linked to oxygen (N···H-O) or nitrogen (N-H···O) [32,33,46,60] atoms and even being in the middle of both (O⁻···H···N⁺) [60,61].

For a prototropic acid-base-system HA in equilibrium, its equilibrium constant K_a is expressed by Equation (1), which after logarithms becomes the Henderson-Hasselbalch Equation (2):

$$K_a = \frac{[H^+][A^-]}{[HA]} \tag{1}$$

$$pH = pK_a + \log\frac{[A^-]}{[HA]} \tag{2}$$

Equation (2) is directly related to the chemical shifts of active nuclei in NMR, which are dependent on *pH* changes, this leads to Equation (3):

$$pH = pK_a + \log\frac{\delta_{max} - \delta_{obs}}{\delta_{obs} - \delta_{min}} \tag{3}$$

The *pKa* is experimentally obtained, using the tabulation of $\log[(\delta_{max} - \delta_{obs})/(\delta_{obs} - \delta_{min})]$ against pH, where δ_{min} and δ_{max} are the chemical shifts in the inflection points in the titration curve, while δ_{obs} is the observed chemical shift during the course of the titration, so the equilibrium point is at point zero, which corresponds to *pH = pKa* [44,62–67]. This method has been extensively used because of its simplicity, however is limited by variability in *pH* readings and accuracy in measuring the volumes of the titrant.

Polster and Lachmann postulated the Gibbs triangle method, which later emerged as the absorbance diagram (A-diagram) or chemical shift diagram (δ-diagram), depending on the spectrometry used for the analysis of data from a titration, for the study of acid-base systems [62,68]. This method allows the evaluation of the quotient of acidity constants (*ΔKa*) of two or more compounds, mainly in diprotic and polyprotic acid-base systems [68], on the bases of a ratio of distances from the Gibbs triangle which is independent of *pH* readings [68].

Later, Perrin *et al.* [69–72] also developed a mathematical model for the determination of *ΔKa* for mixtures of isomers in equilibrium with independency from the *pH* readings by drawing δ-diagrams also, so this model can be applied to the analysis of acid-base equilibrium mainly in monoprotic systems. Then for two acids HA and HB, the quotient of their acidity constants *ΔKa*, can be measured by the variation in chemical shifts due to changes in the acidity of the systems:

$$\Delta K_{\alpha} = \frac{K_a^{HA}}{K_a^{HB}} = \frac{[A^-][HB]}{[HA][B^-]} \tag{4}$$

Equation (4), written in terms of chemical shifts when *ΔKa* ≠ 1, allows the evaluation of *ΔKa* as the slope of a straight line, Equation (5):

$$(\delta_b - \delta_{B°})(\delta_{AH} - \delta_a) = \Delta K_{\alpha}(\delta_a - \delta_{A°})(\delta_{BH} - \delta_b) \tag{5}$$

where $\delta_{A°}$, $\delta_{B°}$ are the chemical shifts from species at the start of the titration, δ_a, δ_b are the chemical shifts observed during the titration, and δ_{HA}, δ_{HB} are the chemical shifts from species at the end of the titration.

In this contribution, both the Perrin and Polster-Lachmann models are applied to the study of intramolecular hydrogen bonds that involve prototropic equilibrium with the aim to find with accuracy and selectivity the position of the proton on the oxygen or nitrogen atoms. The model compounds were a set of Schiff base derivatives of 5-nitrosalicylaldehyde, 5-chlorosalicylaldehyde, 5-bromo-salicylaldehyde, salicylaldehyde, 5-methoxysalicyladehyde and 5-hydroxysalicyladehyde with benzylamine (compounds **1–6**, Figure 1). The substituents were selected in order to cover a broad range of both electrodonating (ED) and electrowithdrawing (EW) groups whose electronic effects could modulate the NHO hydrogen bonding scheme. ^{1}H-NMR spectrometry was used as the titration method.

Figure 1. Schiff base derivatives of **1–6**.

1 R = NO$_2$ **4** R = H
2 R = Cl   **5** R = OCH$_3$
3 R = Br   **6** R = OH
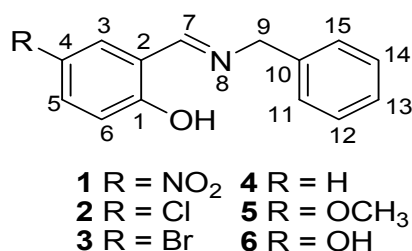
2. Results and Discussion

2.1. NMR Spectra

Synthesized compounds were identified by ^{1}H-, ^{13}C- and ^{15}N-NMR. The ^{1}H-NMR spectra of compounds **1–6** in DMSO-d_6 solution showed remarkable changes in the chemical shift of the acidic proton NHO in the range of 12.53–14.34 ppm, in response to the electronic character of the substituent R. Since a larger value in the chemical shift indicates a greater acidity of the proton, compound **1** has the largest acidity and compound **6** has the lowest acidity. Simultaneously the chemical shift of protons H3, H5, H6 and H7 were affected too.

The ^{13}C spectra of all compounds showed clear shielding and deshielding effects, according to the substituent, mainly from C1 to C7. The chemical shifts of compound **1** were more affected than those of compounds **2–6**, especially the carbon atoms C1 and C4. Compound **1**, the NO$_2$ derivative, showed a chemical shift of 175.8 and 136.9 ppm for C1 and C4, respectively, where C1 is in the range of carbonyl chemical shifts (170 to 200 ppm) while C4 is in the range of nitro Schiff base compounds (130 to 150 ppm). The ^{15}N chemical shift of compound **1** was −162.1 ppm, indicating an average between imine-enamine forms, therefore in this last compound the zwitterionic structure (Scheme 2a) is favored and the hydrogen H8 is localized with the nitrogen atom ($^+$N–H···O).

Scheme 2. Possible resonance and equilibrium structures for compounds **1–6**.
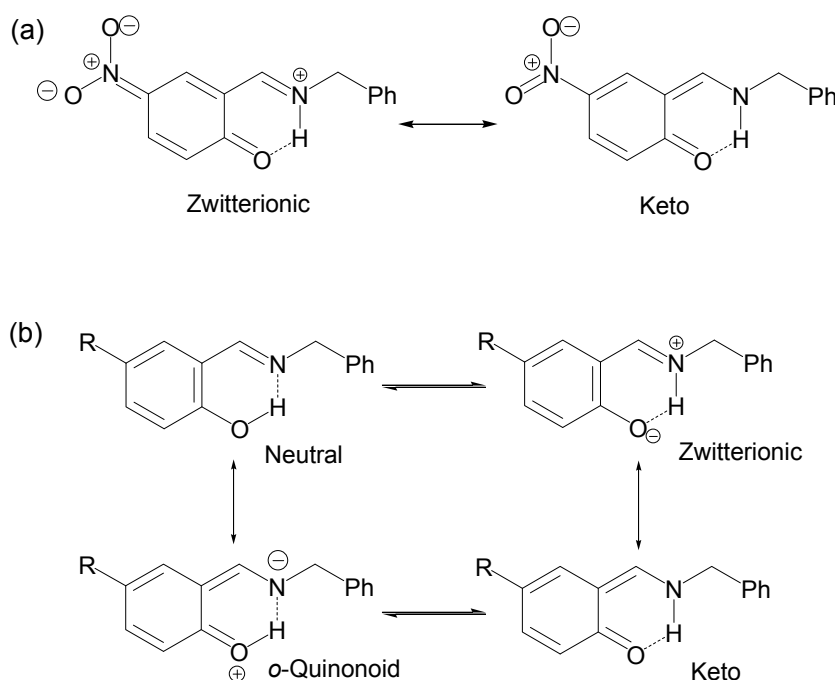
In the case of compounds **2–6** the chemical shifts of C1 appear at lower frequencies from 160.4 to 153.5 ppm, a region characteristic of OH structures (150–160 ppm) and the chemical shifts of the imine C7=N appear from 165.8 to 167.4 ppm, a less significant variation. The ^{15}N chemical shifts for compounds **2–6** were in the range of −79.7 to −81.8 ppm (−50 to −90 ppm for imine), in agreement with a neutral N···H–O tautomeric form with the hydrogen H8 is localized with the oxygen atom (Scheme 2b). The NMR chemical shifts of compounds **1**, **3**, **4** and **5** have already been reported [73]

and are in agreement with the above mentioned results, except for the nitro derivative **1** for which the authors conclude that the N–H tautomer is present in solution instead of the zwitterion form proposed herein.

2.2. NMR Titration

All compounds were titrated in CD_3OD solution with NaOD, and only compound **2** was further titrated with DCl. ^{1}H-NMR spectra were recorded after each aliquot of titrant and simultaneously the *pH* was measured following each recorded spectrum. The resonances of H6 and H9 were used to plot *pH vs.* δ^1H, because these protons were most affected by deprotonation of the labile hydrogen.

Compound **2** was initially titrated with DCl, however hydrolysis occured with the acid titrant and only five ^{1}H spectra and their corresponding *pH* readings could be recorded, so subsequently all compounds were titrated with NaOD (Figure 2A).

Figure 2. (**A**) Titration curve of compounds **2**–**4**; compound **2** was titrated with DCl; only the titration region with NaOD was used to calculate the *pKa* values with the Henderson-Hasselbalch equation; (**B**) δ-Diagram of δ^1_{H6} *vs.* δ^1_{H9} of compounds **2**–**4**; the initial data obtained was not linearized but after using the Perrin model the data became for linearized compounds **2** (Cl), **3** (Br) and **4** (H) to obtain the slope ΔK_{NHO} as shown in Scheme 3.
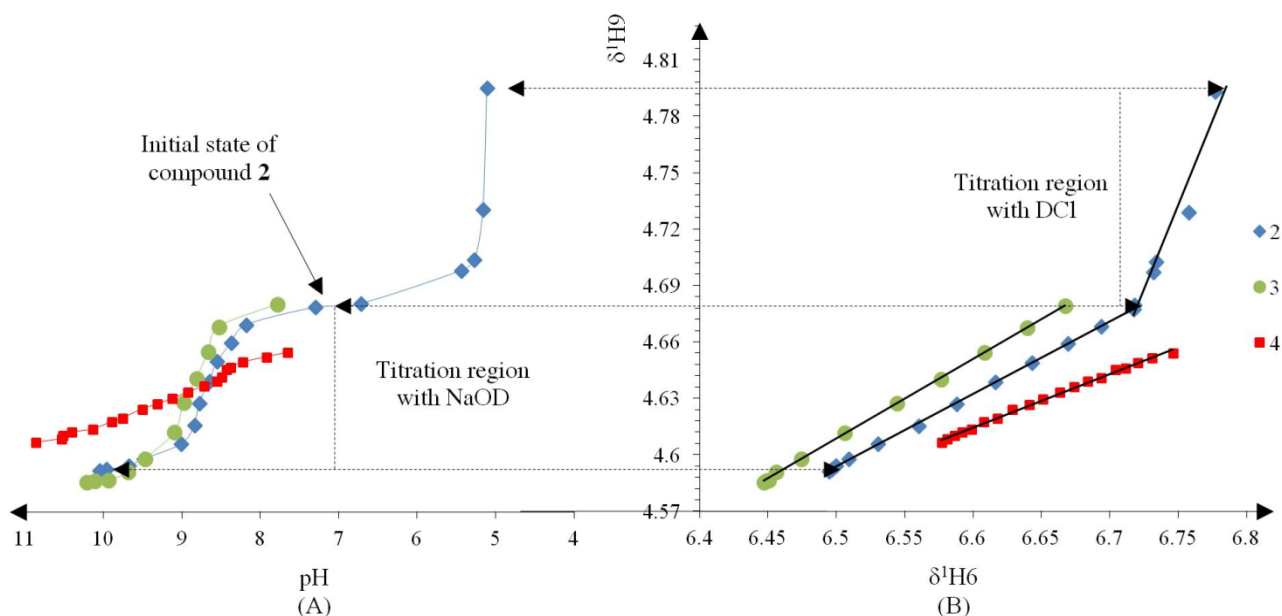
The Henderson-Hasselbalch equation was used to measure *pKa* values of the compounds by a graphical method with plots of *pH* against $log[(\delta_{H9max} - \delta_{H9obs})/(\delta_{H9obs} - \delta_{H9min})]$ (Figure 3) from the titration curve, while ΔK_{NHO} was obtained from the δ-diagram (Figure 2B) using the Perrin model linearization $[(\delta_{H9} - \delta_{H9°})(\delta_{H6}e - \delta_{H6})$ *vs.* $(\delta_{H6} - \delta_{H6°})(\delta_{H9}e - \delta_{H9})]$ for compounds **2**, **3**, **4** and by Polster and Lachmann analysis for compounds **1**, **5** and **6**. Table 1 summarizes the physicochemical parameters obtained by the graphical methods mentioned above.

Figure 3. The experimental pK_a were found using the plot of the Henderson-Hasselbalch equation, when $log[(\delta_{H9max} - \delta_{H9obs})/(\delta_{H9obs} - \delta_{H9min})] = 0$ then the pH intercept is the pK_a value.
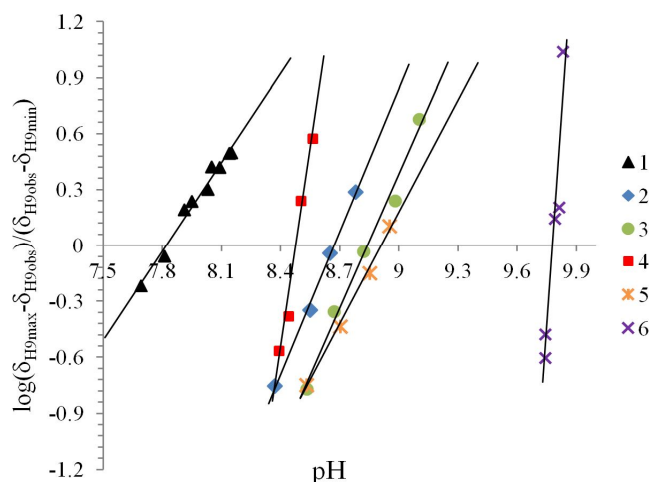

Table 1. Physicochemical parameters of compounds **1–6** at 296.15 ± 1 K in CD_3OD solution.

| Compound	$K_a/10^{-9}$	pK_a	ΔK_{NHO}	ΔpK_{NHO}	$\Delta\Delta G°$ [a]
1	15.1	7.8	1.04(±0.05)	−0.017	−0.097
2	2.13	8.6	1.031(±0.002)	−0.0133	−0.075
3	1.44	8.8	0.986(±0.002)	0.006	0.036
4	3.33	8.4	0.841(±0.005)	0.0754	0.426
5	1.23	8.9	1.021(±0.014)	−0.01	−0.052
6	0.17	9.7	1.02(±0.02)	−0.001	−0.004

[a] $\Delta\Delta G° = -RTln\Delta K_{NHO}$ (kJ mol^{-1} K^{-1}).

The pK_a values obtained by the Henderson-Hasselbalch equation for all compounds were greater than 7 and less than 11, showing that these compounds are weak acids, the pK_a value increases in the order $NO_2 <$ H < Cl < Br < OMe < OH. Only compound **6** showed two pK_a values, the value of 9.7 belongs to NHO and the second value of 9.8 to the phenolic hydroxyl group C4-OH. On the other hand the $\Delta\Delta G°$ values, associated with the prototropic NHO equilibrium, are favored in the order $NO_2 >$ Cl > OMe ≈ OH > Br > H.

Figure 2 shows the titration curve with full pH scale (A) and the δ-diagram (B) of compounds **2** to **4**; only the data region titrated with NaOD was taken for the pK_a value calculation. All compounds should show the same shape of δ-diagram as they were titrated with NaOD. However, the titration curves of compounds **2**, **3** and **4** showed an almost linear behavior, whereas those of compounds **1** and **5** showed one inflection point and those of compound **6** two inflection points (see Supporting Information). These results indicate that the initial structure of compounds **1–6**, at the beginning of the titration, was not the same in agreement with the NMR data discussed above.

On the other hand, the prototropic 1,5-rearrangement (Scheme 3) can be envisaged as composed by two equilibria as depicted by in Figure 2. The quotient of the equilibrium constants K_{HN} and K_{HO} is defined as ΔK_{NHO}, corresponding to the equilibrium constant of the prototropic 1,5-tautomerism. The chemical shifts of H6 and H9 are the most sensitive to changes in the equilibrium positions, thus they were used as probes for K_{HO} and K_{HN} measurements, respectively.

Scheme 3. Equilibria variation in the prototropic 1,5-tautomeric equilibrium. The quotient of the equilibrium constants K_{HN} and K_{HO} is ΔK_{NHO}.
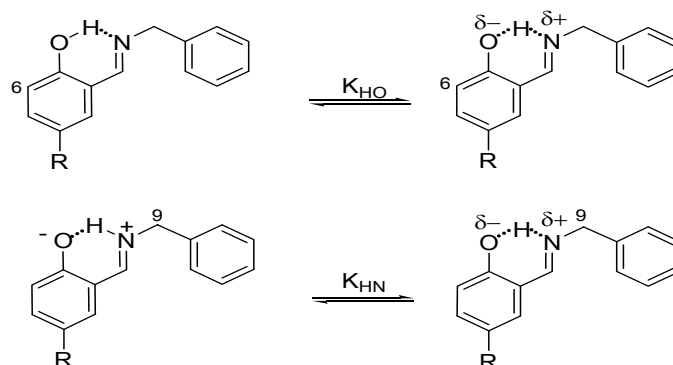

Thus, the ΔK_{NHO} value allows one to establish the position of the NHO equilibrium. Therefore, if the ΔK_{NHO} value is equal to 1 then the system is in equilibrium $N^{\delta+}\cdots H\cdots O^{\delta-}$ and both ΔpK_{NHO} and $\Delta\Delta G°$ are equal to zero; if the value of ΔK_{NHO} is higher than 1, both ΔpK_{NHO} and $\Delta\Delta G°$ are less than zero and labile hydrogen is predominantly positioned on the N atom, $^+N-H\cdots O$; and finally if ΔK_{NHO} is less than 1 then ΔpK_{NHO} and $\Delta\Delta G°$ are greater than zero and therefore the labile hydrogen is predominantly positioned on the O atom, $N\cdots H-O$.

Figure 4. Linearization of ^1H chemical shifts from the δ-diagram for compounds **2**, **3** and **4** by Perrin model. $(\delta_{H9} - \delta_{H9°})(\delta_{H6}e - \delta_{H6}) = \Delta K_{NHO} (\delta_H - \delta_{H6°})(\delta_{H9}e - \delta_{H9})$, ΔK_{NHO} is the slope of the straight line. Compounds **2 (Cl)** $y = 1.031(\pm0.002)x + 8*10^{-5}$, R = 0.996; **3** (Br) $y = 0.986(\pm0.002)x - 2*10^{-5}$, R = 0.994; **4** (H) $y = 0.841(\pm0.005)x - 9*10^{-5}$, R = 0.983.
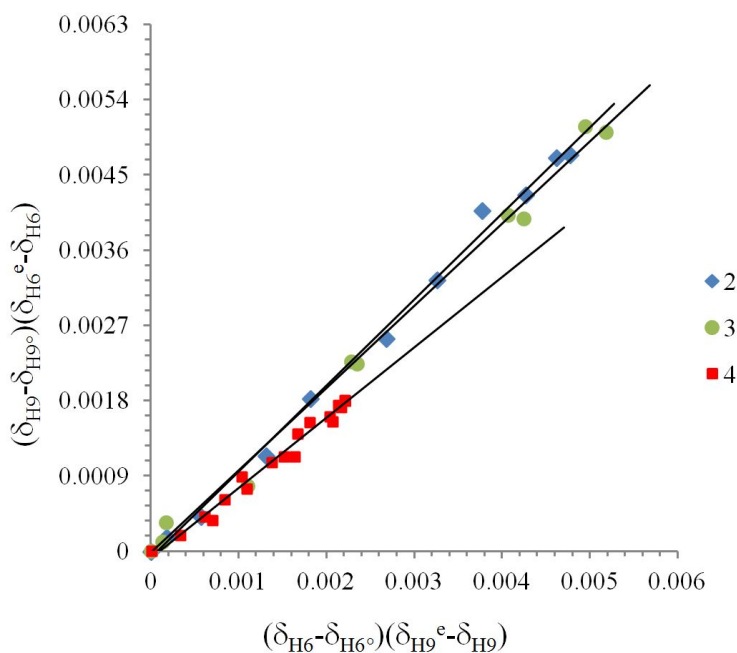
Compounds **2**, **3** and **4** were treated with the Perrin model (Figure 4) for the nonlinear behavior in the δ-diagram. In the case of compounds **1**, **5** and **6** the Polster-Lachmann analysis seems to be more appropriate, because of the shape of the Gibbs triangle taken in the δ-diagram (Figure 5).

Figure 5. Polster-Lachmann analysis of the δ-diagram from compound **5**. Point "A" shows the initial state, point "B" indicates a change on the compound (neutralization point), point "C" the final state and point "BC" is the experimental ΔK_{NHO} of the system. The dotted line A to C shows the shape of a triangle; the dotted line from vertex A to point BC shows the intercept in an ΔK_{NHO} equilibrium point.
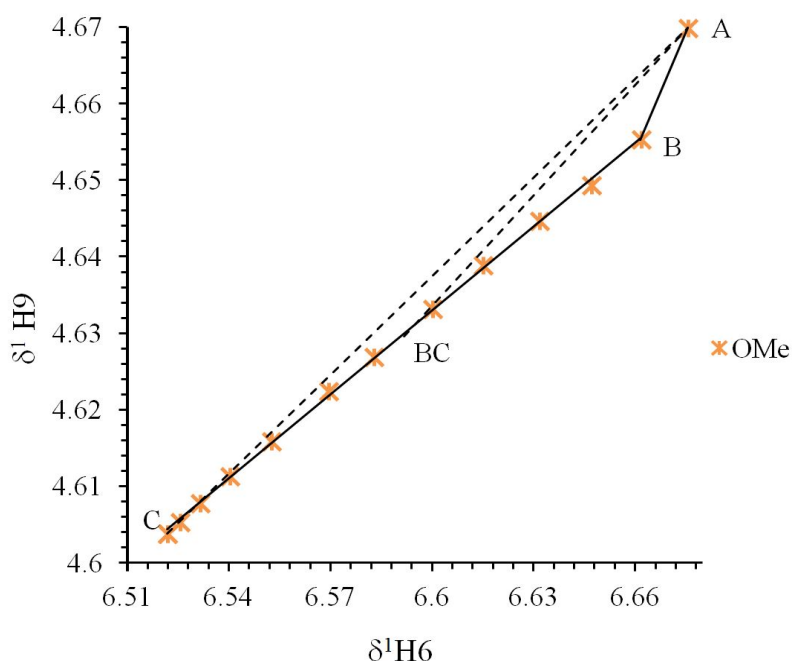

The Polster-Lachmann analysis is based on a ratio of distances established by the Gibbs triangle and the ΔK_{NHO} values are obtained from the chemical shifts of the titration data, hence from points A, B, C and BC in the δ-diagram, in agreement with Equation (6):

$$\Delta K_{NHO} = \frac{K^{HN}}{K^{HO}} = \frac{(BC)(B)}{(BC)(C)} \tag{6}$$

From δ-diagrams, the mechanism occurring in the course of the titration with NaOD, can be proposed (Scheme 4).

Scheme 4. Mechanism proposed during the titration with NaOD; the scheme is according to points in the δ-diagram of Figure 5.
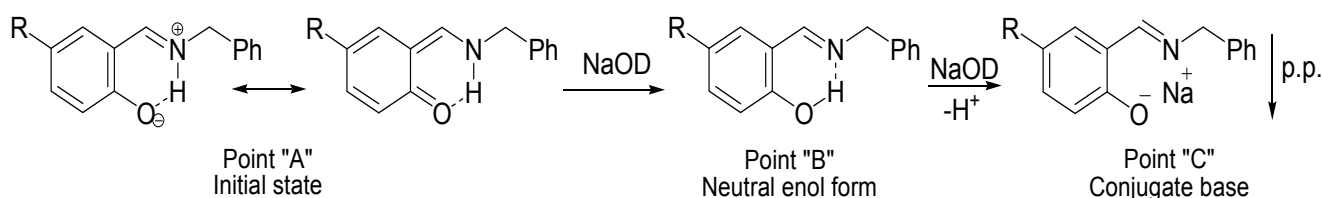
Compounds **1**, **2**, **5** and **6** begin at an initial state as acidic species (Point "A"), with a small increase of *pH*, the intramolecular hydrogen bond equilibrium is shifted from $^+$N-H···O$^-$ to N···H-O, reaching the neutralization point of the solution (Point "B"); then, as long as the *pH* is increased compounds are deprotonated to become into the conjugated bases that precipitate as a salt (Point "C"). In the case of

compounds **3** and **4**, the initial state is at point "B" with the intramolecular hydrogen bond in the N⋯H-O form, the addition of NaOD aliquots only shift the equilibrium to point "C" the conjugate base.

The δ-diagrams show the initial state in all compounds and indicate the most stable species in a methanol solution, so the stability of the NHO intramolecular hydrogen bond is affected by the electronic nature of the substituent as well as solvation of methanol; therefore, the structure of compounds **1**, **5** and **6** with NO_2, OMe and OH substituents, respectively, stabilizes and direct the NHO equilibrium position by both mesomeric and inductive effects, although they have different ΔK_{NHO} values, whereas the halogen substituent in compounds **2** and **3** exert both electronegative and inductive effects; none of such effects are present in compound **4**. Thus from the obtained ΔK_{NHO} values, the predominant NHO equilibrium in compounds **3** and **4** are the neutral N⋯H–O form, while for the rest of the compounds the zwitterionic $^+$N–H⋯O$^-$ form is present (Scheme 2). In the particular case of compound **1**, it is as an imine-enamine tautomeric form in agreement with ^{1}H, ^{13}C and ^{15}N pfg-HMQC spectroscopy mentioned above.

Finally, the obtained ΔK_{NHO} values (Table 1) are very close to the equilibrium point N$^{\delta-}$⋯H$^+$⋯O$^{\delta-}$ ($\Delta K_{NHO} = 1$), which indicate a fast interchange of intramolecular hydrogen bond and the effect produced by both the substituent and the solvent that stabilize the systems in a preferred tautomeric form.

3. Experimental

3.1. General Remarks

Schiff bases **1** to **6** were obtained by condensation of the appropriate aromatic *ortho*-hydroxyaldehyde with benzylamine in toluene at 25 °C (Scheme 5). Solids products were filtered and dried under a *vacuum*. Compound **4** was a liquid and the excess of toluene was eliminated under vacuum. ^{1}H and ^{13}C-NMR spectra were recorded in DMSO-d_6 on a JEOL ECA-500 spectrometer (^{1}H, 500.1 MHz; ^{13}C, 125.7 MHz; ^{15}N, 50.7 MHz) and the ^{15}N chemical shifts were obtained by correlation of ^{1}H,^{15}N pfg-HMQC (see Supporting Information).

Scheme 5. Synthesis of Schiff bases.

1 R = NO_2 **4** R = H
2 R = Cl   **5** R = OCH_3
3 R = Br   **6** R = OH
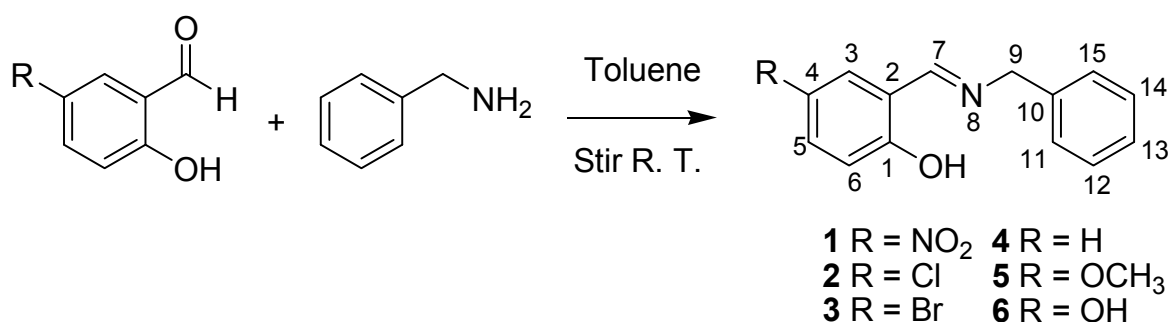
(E)-2-((Benzylimino)methyl)-4-nitrophenol (**1**). Compound **1** was prepared as reported [73] by condensation of 5-nitrosalicylaldehyde (0.5 g, 2.99 mmol) with benzylamine (0.32 g, 0.32 mL, 2.99 mmol) in toluene at room temperature (25 °C) and with a stirring time of 5 min. ^{1}H-NMR (DMSO-d_6): δ = 8.42 (*d*, $^4J_{H,H}$ = 2.9 Hz, 1H, H3), 8.02 (*dd*, $^3J_{H,H}$ = 9.5, $^4J_{H,H}$ = 3.0 Hz, 1H, H5), 6.65 (*d*, $^3J_{H,H}$ = 9.5 Hz, 1H, H6), 8.86 (*s*, 1H, H7), 4.84 (*s*, 2H, H9), 7.28–7.37 (*m*, 5H, H11-H15), 14.3 (broad signal, 1H,

NHO) ppm. ^{13}C-NMR (DMSO-d_6): δ = 175.8 (*s*, 1C, C1), 115.0 (*s*, 1C, C2), 132.1 (*s*, 1C, C3), 136.9 (*s*, 1C, C4), 129.5 (*s*, 1C, C5), 122.2 (*s*, 1C, C6), 167.4 (*s*, 1C, C7), 57.2 (*s*, 1C, C9), 135.5 (*s*, 1C, C10), 129.3 (*s*, 2C, C11, C15), 128.6 (*s*, 2C, C12, C14), 128.5 (*s*, 1C, C13) ppm. ^{15}N-NMR (DMSO-d_6): δ = −162.1 (*s*, 1N, N8), −9.5 (*s*, 1N, N4) ppm.

(E)-2-((Benzylimino)methyl)-4-chlorophenol (**2**). Compound **2** was prepared by condensation of 5-chlorosalicylaldehyde (0.5 g, 3.19 mmol) with benzylamine (0.34 g, 0.34 mL, 3.19 mmol) in toluene at room temperature (25 °C) and with a stirring time of 5 min. Yield 0.73 g (93%). m.p. 359–360 K. FT-IR (ATR, cm^{-1}): 1628 (C=N), 1573 (asymmetrical C=C-O-H stretch), 1479 (symmetrical C=C-O-H stretch), 3069 (intramolecular hydrogen bonding N···H-O, as a weak broad band). LC-MS-TOF in HPLC-methanol solution, *m/z* (%) calculated: 246.0686 (100); found: 246.0680 (100) [M+H]$^+$, empirical formula C$_{14}$H$_{13}$NOCl. ^{1}H-NMR (DMSO-d_6): δ = 7.53 (*d*, $^4J_{\text{H,H}}$ = 2.7 Hz, 1H, H3), 7.31 (*dd*, $^3J_{\text{H,H}}$=8.7, $^4J_{\text{H,H}}$ = 2.7 Hz, 1H, H5), 6.87 (*d*, $^3J_{\text{H,H}}$ = 8.8 Hz, 1H, H6), 8.64 (*s*, 1H, H7), 4.76 (*s*, 2H, H9), 7.23–7.34 (*m*, 5H, H11-H15), 13.4 (broad signal, 1H, NHO) ppm. ^{13}C-NMR (DMSO-d_6): δ = 160.0 (*s*, 1C, C1), 120.2 (*s*, 1C, C2), 131.1 (*s*, 1C, C3), 122.5 (*s*, 1C, C4), 132.5 (*s*, 1C, C5), 119.0 (*s*, 1C, C6), 165.8 (*s*, 1C, C7), 62.4 (*s*, 1C, C9), 138.8 (*s*, 1C, C10), 129.1 (*s*, 2C, C11, C15), 128.3 (*s*, 2C, C12, C14), 127.7 (*s*, 1C, C13) ppm. ^{15}N-NMR (DMSO-d_6): δ = −80.5 (*s*, 1N, N8) ppm.

(E)-2-((Benzylimino)methyl)-4-bromophenol (**3**). Compound **3** was prepared as reported [73] by condensation of 5-bromosalicylaldehyde (0.5 g, 2.48 mmol) with benzylamine (0.26 g, 0.27 mL, 2.48 mmol) in toluene at room temperature of 25 °C and with a stirring time of 5 min. ^{1}H-NMR (DMSO-d_6): δ = 7.64 (*d*, $^4J_{\text{H,H}}$ = 2.5 Hz, 1H, H3), 7.41 (*dd*, $^3J_{\text{H,H}}$ = 8.7 and $^4J_{\text{H,H}}$ = 2.7 Hz, 1H, H5), 6.82 (*d*, $^3J_{\text{H,H}}$ = 8.7 Hz, 1H, H6), 8.62 (*s*, 1H, H7), 4.75 (*s*, 2H, H9), 7.22–7.33 (*m*, 5H, H11-H15), 13.5 (broad signal, 1H, NHO) ppm. ^{13}C-NMR (DMSO-d_6): δ = 160.4 (*s*, 1C, C1), 120.9 (*s*, 1C, C2), 134.0 (*s*, 1C, C3), 109.8 (*s*, 1C, C4), 135.3 (*s*, 1C, C5), 119.5 (*s*, 1C, C6), 165.7 (*s*, 1C, C7), 62.4 (*s*, 1C, C9), 138.8 (*s*, 1C, C10), 129.1 (*s*, 2C, C11, C15), 128.3 (*s*, 2C, C12, C14), 127.8 (*s*, 1C, C13) ppm. ^{15}N-NMR (DMSO-d_6): δ = −81.8 (*s*, 1N, N8) ppm.

(E)-2-((Benzylimino)methyl)phenol (**4**). Compound **4** was prepared as reported [73] by condensation of salicylaldehyde (0.5 g, 0.42 mL, 4.09 mmol) with benzylamine (0.43 g, 0.44 mL, 4.09 mmol) in toluene at room temperature (25 °C) and with a stirring time of 5 min. ^{1}H-NMR (DMSO-d_6): δ = 7.44 (*dd*, $^3J_{\text{H,H}}$ = 7.5, $^4J_{\text{H,H}}$ = 1.7 Hz, 1H, H3), 6.87 (*td*, $^3J_{\text{H,H}}$ = 7.4, $^3J_{\text{H,H}}$ = 8.3 and $^4J_{\text{H,H}}$ = 0.9, 1H, H4), 7.30 (*t, d*, $^3J_{\text{H,H}}$ = 7.4, $^3J_{\text{H,H}}$ = 8.2 and $^4J_{\text{H,H}}$ = 1.7 Hz, 1H, H5), 6.85 (*dd*, $^3J_{\text{H,H}}$ = 8.2 and $^4J_{\text{H,H}}$ = 1.0 Hz, 1H, H6), 8.67 (*s*, 1H, H7), 4.76 (*s*, 2H, H9), 7.23–7.34 (*m*, 5H, H11-H15), 13.4 (*s*, 1H, NHO) ppm. ^{13}C-NMR (DMSO-d_6): δ = 161.2 (*s*, 1C, C1), 119.2 (*s*, 1C, C2), 132.3 (*s*, 1C, C3), 119.1 (*s*, 1C, C4), 132.9 (*s*, 1C, C5), 117.0 (*s*, 1C, C6), 166.8 (*s*, 1C, C7), 62.7 (*s*, 1C, C9), 139.0 (*s*, 1C, C10), 129.0 (*s*, 2C, C11, C15), 128.2 (*s*, 2C, C12, C14), 127.6 (*s*, 1C, C13) ppm. ^{15}N-NMR (DMSO-d_6): δ = −81.7 (*s*, 1N, N8) ppm.

S1-5 (E)-2-((Benzylimino)methyl)-4-methoxyphenol (**5**). Compound **5** was prepared as reported [73] by condensation of 5-methoxysalicylaldehyde (0.5 g, 0.40 mL, 3.28 mmol) with benzylamine (0.35 g, 0.35 mL, 3.28 mmol) in toluene at room temperature (25 °C) and with a stirring time of 5 min. ^{1}H-NMR (DMSO-d_6): δ = 7.04 (*d*, $^4J_{\text{H,H}}$ = 3.1 Hz, 1H, H3), 6.95 (*dd*, $^3J_{\text{H,H}}$ = 9.0 and $^4J_{\text{H,H}}$ = 3.1 Hz,

1H, H5), 6.87 (*d*, $^3J_{H,H}$ = 9.0, 1H, H6), 8.58 (*s*, 1H, H7), 4.74 (*s*, 2H, H9), 7.22–7.34 (*m*, 5H, H11-H15), 3.70 (*s*, 3H, H16), 12.8 (*s*, 1H, NHO) ppm. ^{13}C-NMR (DMSO-d_6): δ= 155.0 (*s*, 1C, C1), 119.0 (*s*, 1C, C2), 115.4 (*s*, 1C, C3), 152.2 (*s*, 1C, C4), 119.8 (*s*, 1C, C5), 117.7 (*s*, 1C, C6), 166.6 (*s*, 1C, C7), 62.9 (*s*, 1C, C9), 139.1 (*s*, 1C, C10), 129.0 (*s*, 2C, C11, C15), 128.2 (*s*, 2C, C12, C14), 127.6 (*s*, 1C, C13), 55.9 (*s*, 1C, C16) ppm. ^{15}N-NMR (DMSO-d_6): δ = −79.8 (*s*, 1N, N8) ppm.

(E)-2-((Benzylimino)methyl)benzene-1,4-diol (**6**). Compound **6** was prepared by condensation of 5-hydroxysalicylaldehyde (0.5 g, 3.62 mmol) with benzylamine (0.38 g, 0.39 mL, 3.62 mmol) in toluene at room temperature of 25 °C and with a stirring time of 5 min. Yield 0.73 g (89%). m.p. 397–399 K. FT-IR (ATR, cm^{-1}): 1641 (C=N), 1601 (asymmetrical C=C-O-H stretch), 1496 (symmetrical C=C-O-H stretch), 3311 (free phenolic O-H medium broad band), 3054 (intramolecular hydrogen bonding N···H-O, as a weak broad band). LC-MS-TOF in HPLC-grade methanol, *m/z* (%) calculated: 228.1025 (100); found: 228.1022 (100) [M+H]$^+$, empirical formula $C_{14}H_{14}NO_2$. ^{1}H-NMR (DMSO-d_6): δ= 6.83 (*d*, $^4J_{H,H}$ = 3.0 Hz, 1H, H3), 6.76 (*dd*, $^3J_{H,H}$ = 8.8, $^4J_{H,H}$ = 3.0 Hz, 1H, H5), 6.68 (*d*, $^3J_{H,H}$ = 8.9, 1H, H6), 8.58 (*s*, 1H, H7), 4.74 (*s*, 1H, H9), 7.23–7.34 (*m*, 5H, H11-H15), 9.00 (*s*, 1H, C4-OH), 12.5 (*s*, 1H, NHO) ppm. ^{13}C-NMR (DMSO-d_6): δ= 153.5 (*s*, 1C, C1), 119.1 (*s*, 1C, C2), 117.0 (*s*, 1C, C3), 149.9 (*s*, 1C, C4), 120.5 (*s*, 1C, C5), 117.4 (*s*, 1C, C6), 166.8 (*s*, 1C, C7), 62.8 (*s*, 1C, C9), 139.3 (*s*, 1C, C10), 129.1 (*s*, 2C, C11, C15), 128.3 (*s*, 2C, C12, C14), 127.6 (*s*, 1C, C13) ppm. ^{15}N-NMR (DMSO-d_6): δ= −79.7 (*s*, 1N, N8) ppm.

3.2. Sample Preparation, Titrant Solution and pH Meter

Solutions of compounds **1–6** (0.06–0.10 M) in CD$_3$OD (0.4–0.5 mL) and 1,4-dioxane as internal reference (0.5–1.5 μL, δ$_H$ 3.53), were prepared in resonance tubes. The NaOD titrant solution, was prepared to 1.4 and 4.8% (v/v) from NaOD/D$_2$O (40%) in CD$_3$OD, while the DCl solution was prepared to 5% from DCl/D$_2$O (70%) in CD$_3$OD. The glass electrode was filled with a KCl standard solution and calibrated with phosphate buffer pH 7.0 and 4.0.

3.3. NMR Spectrometric Titration

The ^{1}H-NMR spectra were recorded in CD$_3$OD on a JEOL ECA-500 spectrometer at room temperature of 295.15 ± 1 K (22 ± 1 °C). An initial ^{1}H-NMR spectrum of the solutions was recorded and assigned as initial value for the titration. Subsequently the solutions were titrated with aliquots of the NaOD/D$_2$O solution base (3.0 μL), until invariant changes in the chemical shifts were observed; each ^{1}H-NMR spectrum as well as the corresponding *pH* reading were recorded simultaneously, after the addition of the base. Only compound **2** was further titrated with DCl (5%), to observe the behavior of the system at acidic pH.

3.4. NMR Titration Graphics (Figures 6–11)

Figure 6. (**A**) titration curve (pH *vs.* δ^1H9); (**B**) δ-diagram with Polster-Lachmann analysis (δ^1H6 *vs.* δ^1H9) and (**C**) plot of the semilogarithmic Henderson-Hasselbalch equation (pH *vs.* $\log[(\delta_{H9max} - \delta_{H9obs})/(\delta_{H9obs} - \delta_{H9min})]$) of compound **1** (R = NO$_2$).
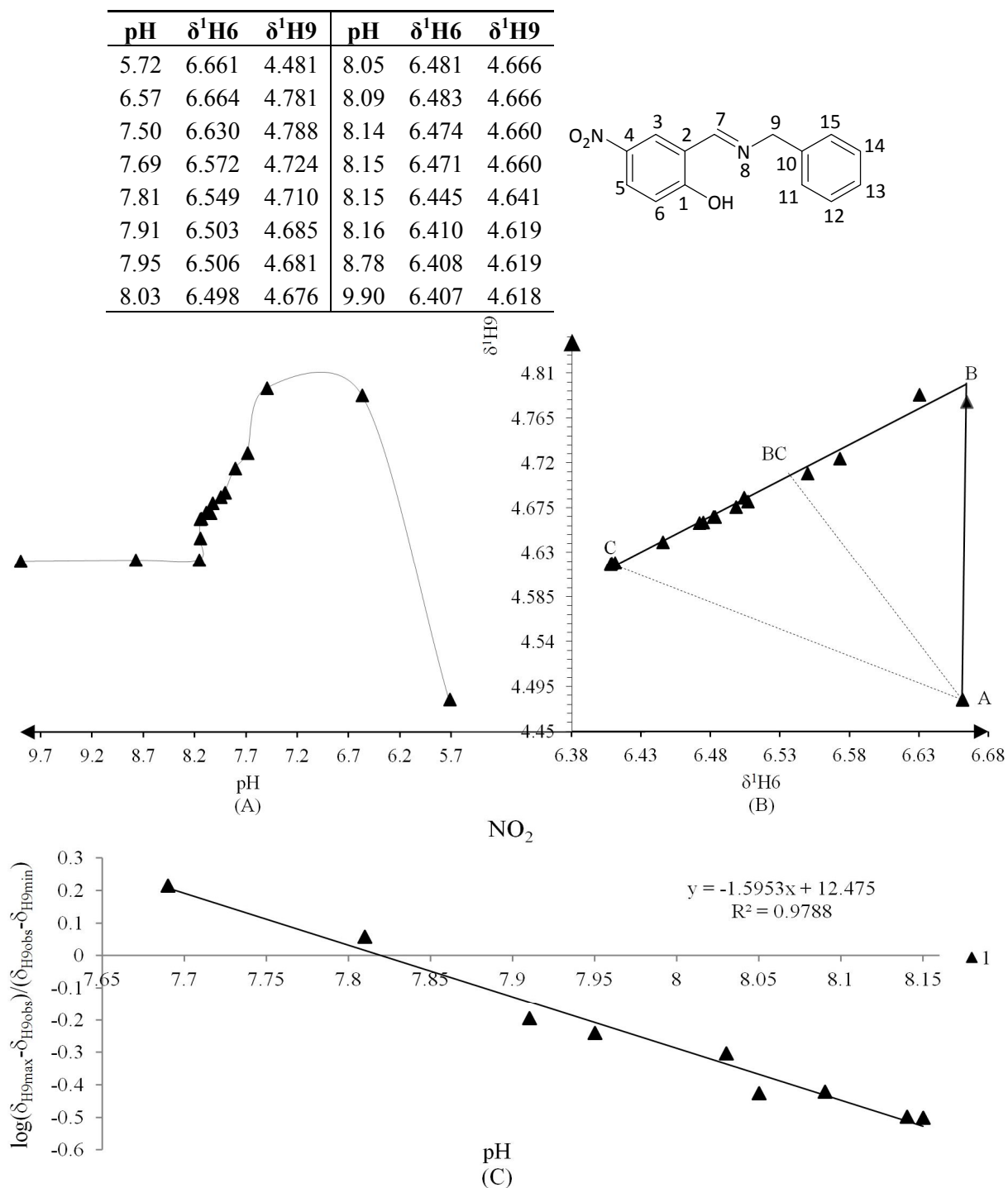
pH	δ^1H6	δ^1H9	pH	δ^1H6	δ^1H9
5.72	6.661	4.481	8.05	6.481	4.666
6.57	6.664	4.781	8.09	6.483	4.666
7.50	6.630	4.788	8.14	6.474	4.660
7.69	6.572	4.724	8.15	6.471	4.660
7.81	6.549	4.710	8.15	6.445	4.641
7.91	6.503	4.685	8.16	6.410	4.619
7.95	6.506	4.681	8.78	6.408	4.619
8.03	6.498	4.676	9.90	6.407	4.618

y = -1.5953x + 12.475
R² = 0.9788

Figure 7. (**A**) titration curve (pH *vs.* δ^1H9); (**B**) δ-diagram with Perrin model analysis (δ^1H6 *vs.* δ^1H9) and (**C**) plot of the semilogarithmic Henderson-Hasselbalch equation (pH *vs.* $\log[(\delta_{H9max} - \delta_{H9obs})/(\delta_{H9obs} - \delta_{H9min})]$) of compound **2** (R = Cl). Only compound **2** was titrated with DCl solution.

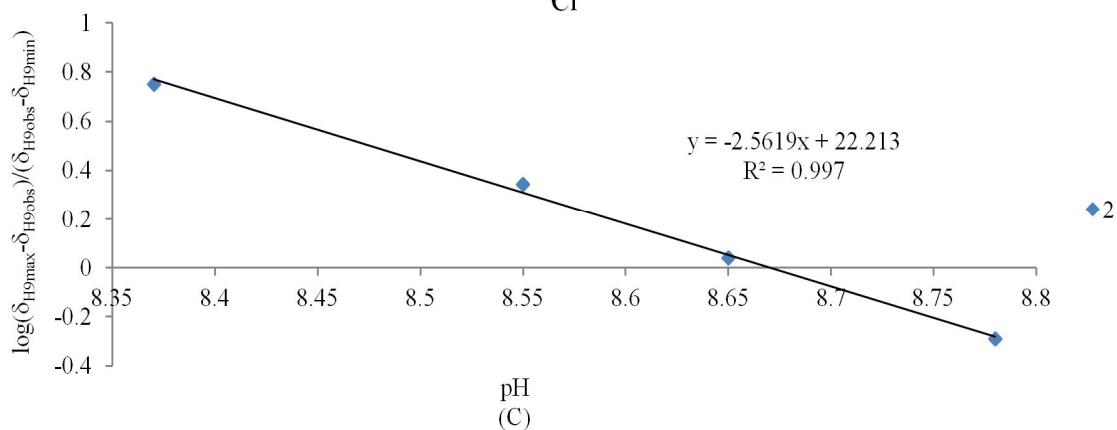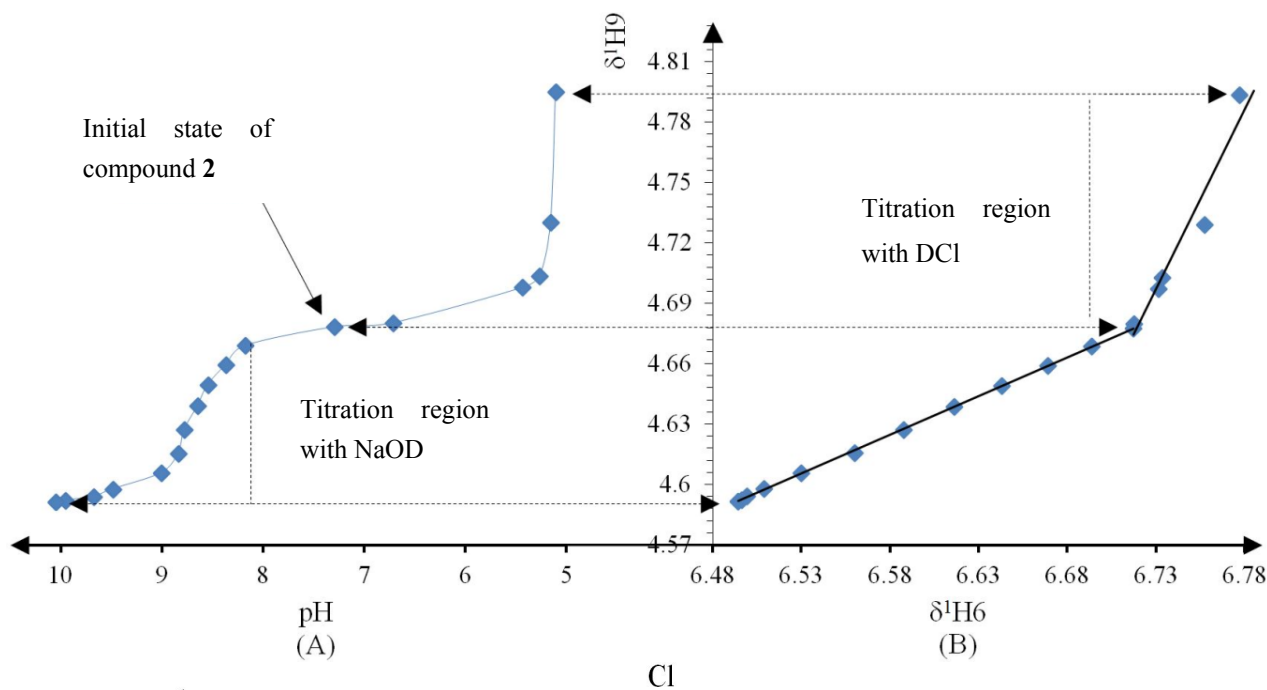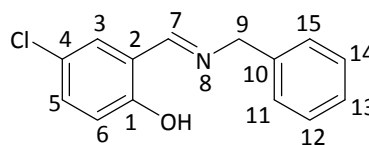| pH	δ^1H6	δ^1H9	pH	δ^1H6	δ^1H9
5.11	6.777	4.793	8.65	6.616	4.638
5.16	6.757	4.729	8.78	6.587	4.627
5.27	6.733	4.702	8.84	6.560	4.615
5.44	6.731	4.697	9.01	6.530	4.605
6.72	6.717	4.679	9.49	6.508	4.597
7.30	6.717	4.677	9.68	6.499	4.594
8.18	6.693	4.668	9.96	6.496	4.592
8.37	6.669	4.659	10.05	6.494	4.591
8.55	6.643	4.649			

Figure 8. (**A**) titration curve (pH *vs.* δ^1H9); (**B**) δ-diagram with Perrin model analysis (δ^1H6 *vs.* δ^1H9) and (**C**) plot of the semilogarithmic Henderson-Hasselbalch equation (pH *vs.* $\log[(\delta_{H9max} - \delta_{H9obs})/(\delta_{H9obs} - \delta_{H9min})]$) of compound **3** (R = Br).

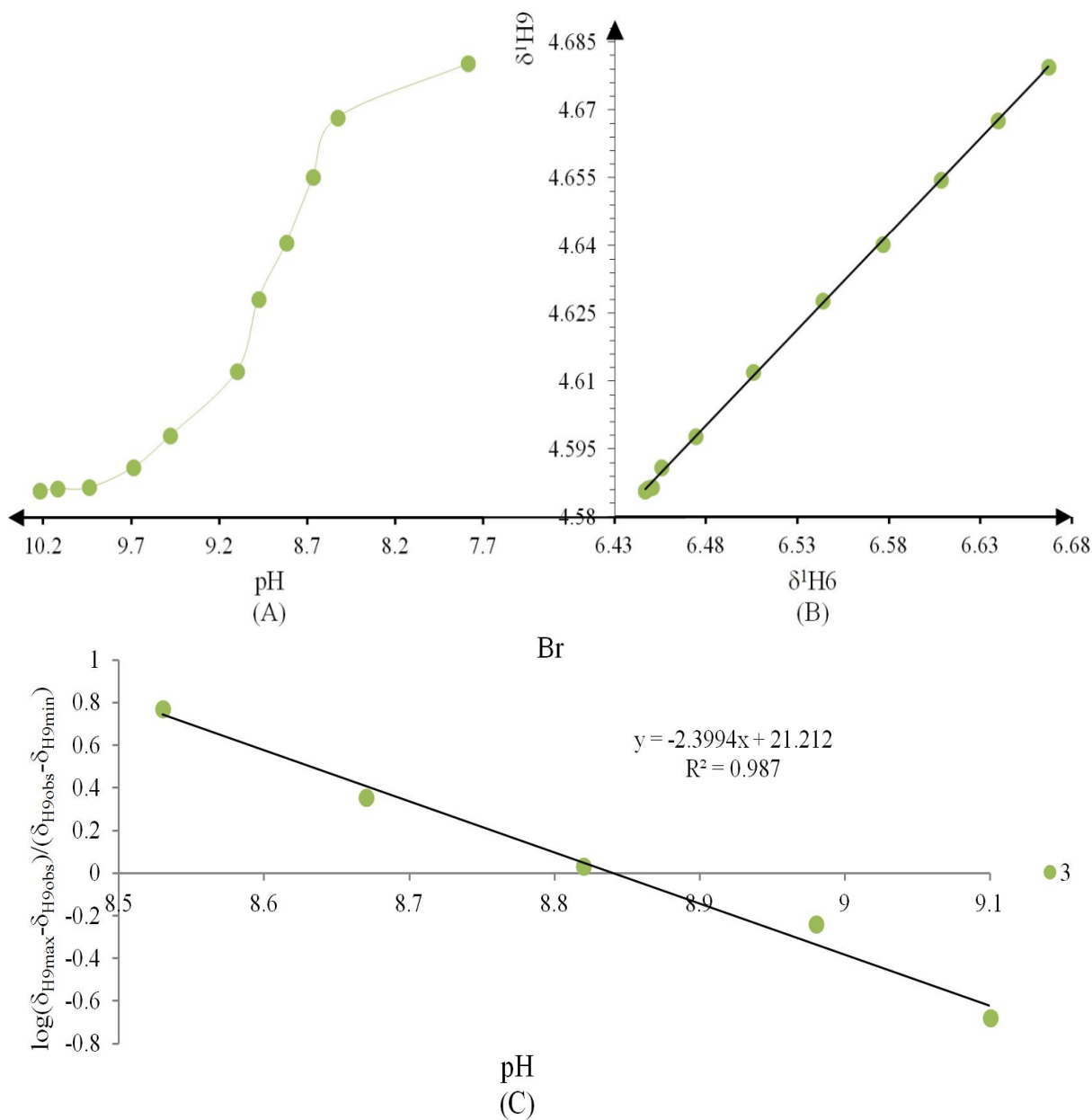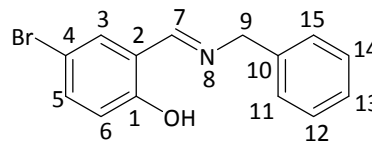| pH	δ^1H6	δ^1H9	pH	δ^1H6	δ^1H9
7.79	6.667	7.269	9.48	6.474	7.027
8.53	6.639	7.234	9.69	6.455	7.004
8.67	6.608	7.194	9.94	6.450	6.998
8.82	6.576	7.154	10.12	6.448	6.995
8.98	6.543	7.114	10.22	6.446	6.993
9.10	6.505	7.066			

Figure 9. (**A**) titration curve (pH *vs.* δ^1H9); (**B**) δ-diagram with Perrin model analysis (^{1}H6 *vs.* ^{1}H9) and (**C**) plot of the semilogarithmic Henderson-Hasselbalch equation (pH *vs.* $\log[(\delta_{H9max} - \delta_{H9obs})/(\delta_{H9obs} - \delta_{H9min})]$)of compound **4** (R = H).

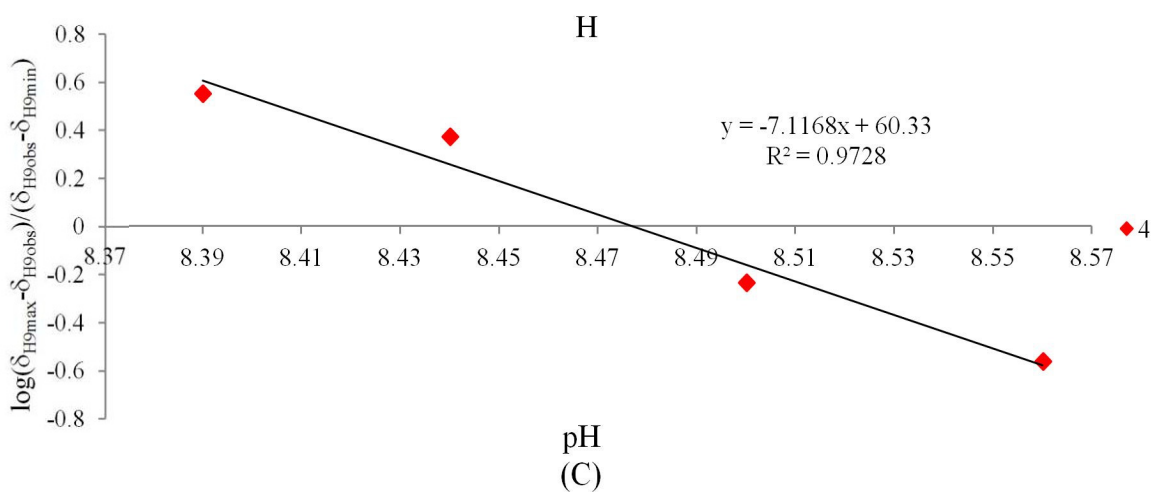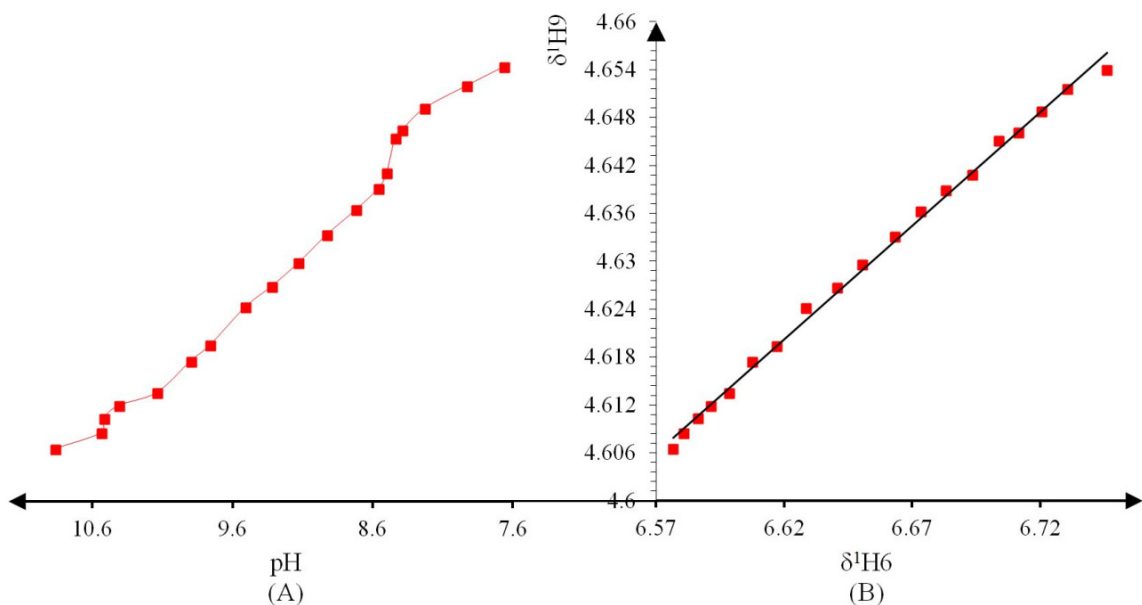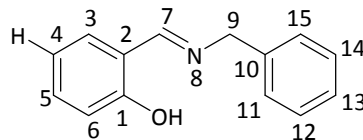| pH	δ^1H6	δ^1H9	pH	δ^1H6	δ^1H9
7.66	6.746	4.654	9.32	6.640	4.626
7.93	6.730	4.651	9.51	6.628	4.624
8.23	6.720	4.648	9.76	6.617	4.619
8.39	6.711	4.646	9.90	6.607	4.617
8.44	6.703	4.645	10.14	6.598	4.613
8.50	6.693	4.640	10.41	6.591	4.611
8.56	6.683	4.638	10.52	6.586	4.610
8.72	6.673	4.636	10.54	6.581	4.608
8.93	6.663	4.633	10.87	6.576	4.606
9.13	6.650	4.629			

(A) (B)

$y = -7.1168x + 60.33$
$R^2 = 0.9728$

pH
(C)

Figure 10. (**A**) titration curve (pH *vs.* δ^1H9); (**B**) δ-diagram with Polster-Lachmann analysis (δ^1H6 *vs.* δ^1H9) and (**C**) plot of the semilogarithmic Henderson-Hasselbalch equation (pH *vs.* $\log[(\delta_{H9max} - \delta_{H9obs})/(\delta_{H9obs} - \delta_{H9min})]$) of compound **5** (R = OMe).

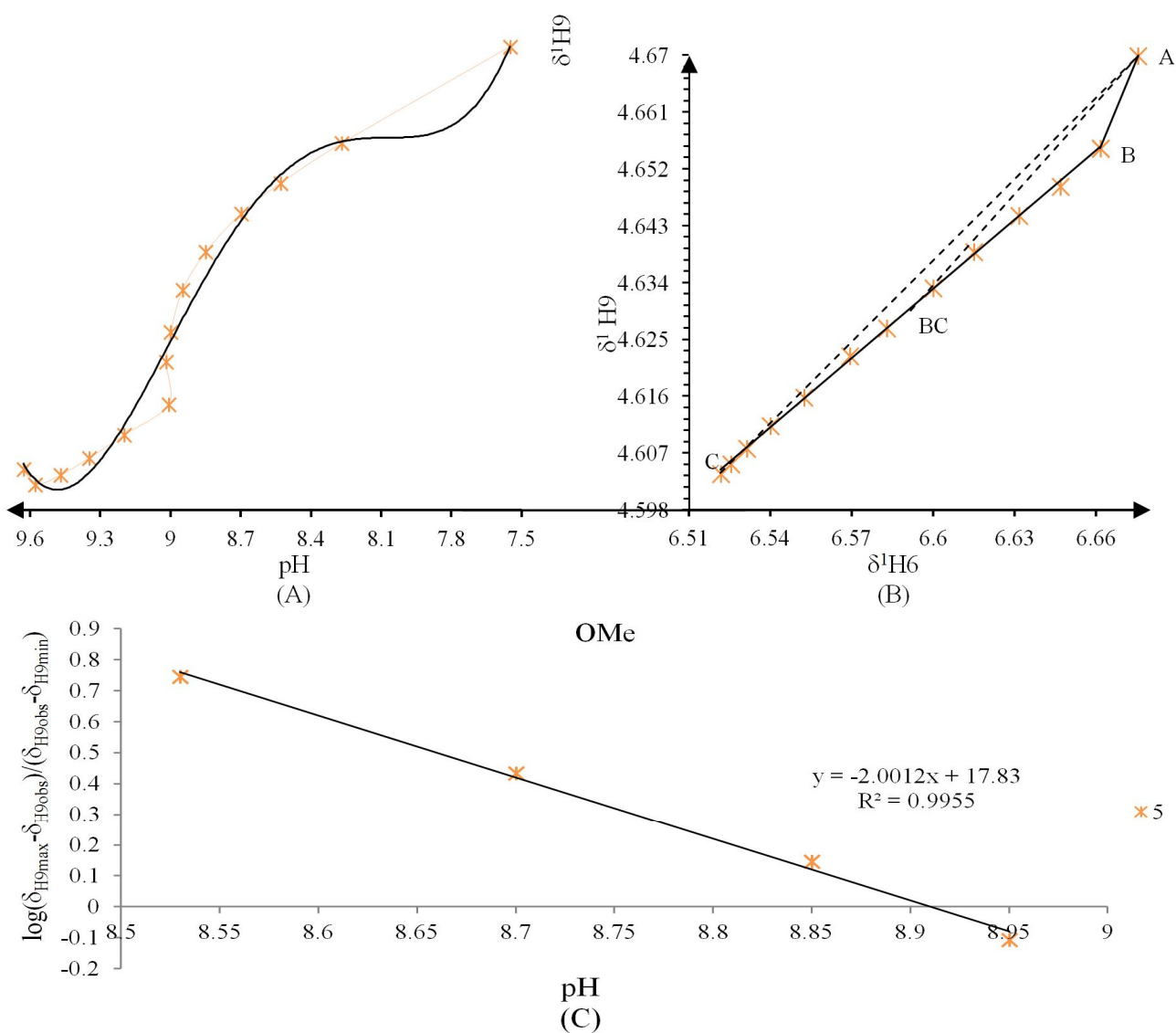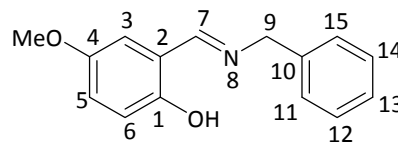| pH	δ^1H6	δ^1H9	pH	δ^1H6	δ^1H9
7.55	6.675	4.669	9.02	6.569	4.622
8.27	6.661	4.655	9.01	6.552	4.615
8.53	6.646	4.649	9.20	6.540	4.611
8.70	6.631	4.644	9.35	6.531	4.607
8.85	6.615	4.638	9.47	6.525	4.605
8.95	6.599	4.633	9.58	6.521	4.603
9.00	6.582	4.627	9.63	6.518	4.606

(A)

(B)

(C)

Figure 11. (**A**) titration curve (pH *vs.* δ^1H5); (**B**) δ-diagram with Polster-Lachmann analysis (δ^1H6 *vs.* δ^1H5) and (**C**) plot of the semilogarithmic Henderson-Hasselbalch equation (pH *vs.* log[($\delta_{H5max} - \delta_{H5obs}$)/($\delta_{H5obs} - \delta_{H5min}$)])of compound **6** (R = OH) calculating the *pKa2*. The *pKa2* value belong to deprotonation of intramolecular hydrogen bond N···H-O, whereas *pKa3* correspond to free phenolic C4-OH. For this compound the plot of δ-diagram was done with ^{1}H6 *vs.* ^{1}H5 chemical shifts, since only this correlation showed a system with three slope changes similar to polyprotic system.

pH	δ^1H6	δ^1H5	pH	δ^1H6	δ^1H5
6.41	6.603	6.690	9.69	6.569	6.664
8.85	6.602	6.689	9.77	6.566	6.662
9.58	6.601	6.686	9.92	6.566	6.662
9.76	6.596	6.684	9.99	6.562	6.659
9.80	6.595	6.683	10.04	6.558	6.655
9.83	6.590	6.681	10.04	6.555	6.653
9.84	6.587	6.678	10.03	6.551	6.650
9.85	6.583	6.676	10.02	6.546	6.646
9.84	6.580	6.673	10.02	6.545	6.644
9.68	6.577	6.670	10.03	6.539	6.640
9.68	6.573	6.667	10.01	6.534	6.635

(A)

(B)

(C)
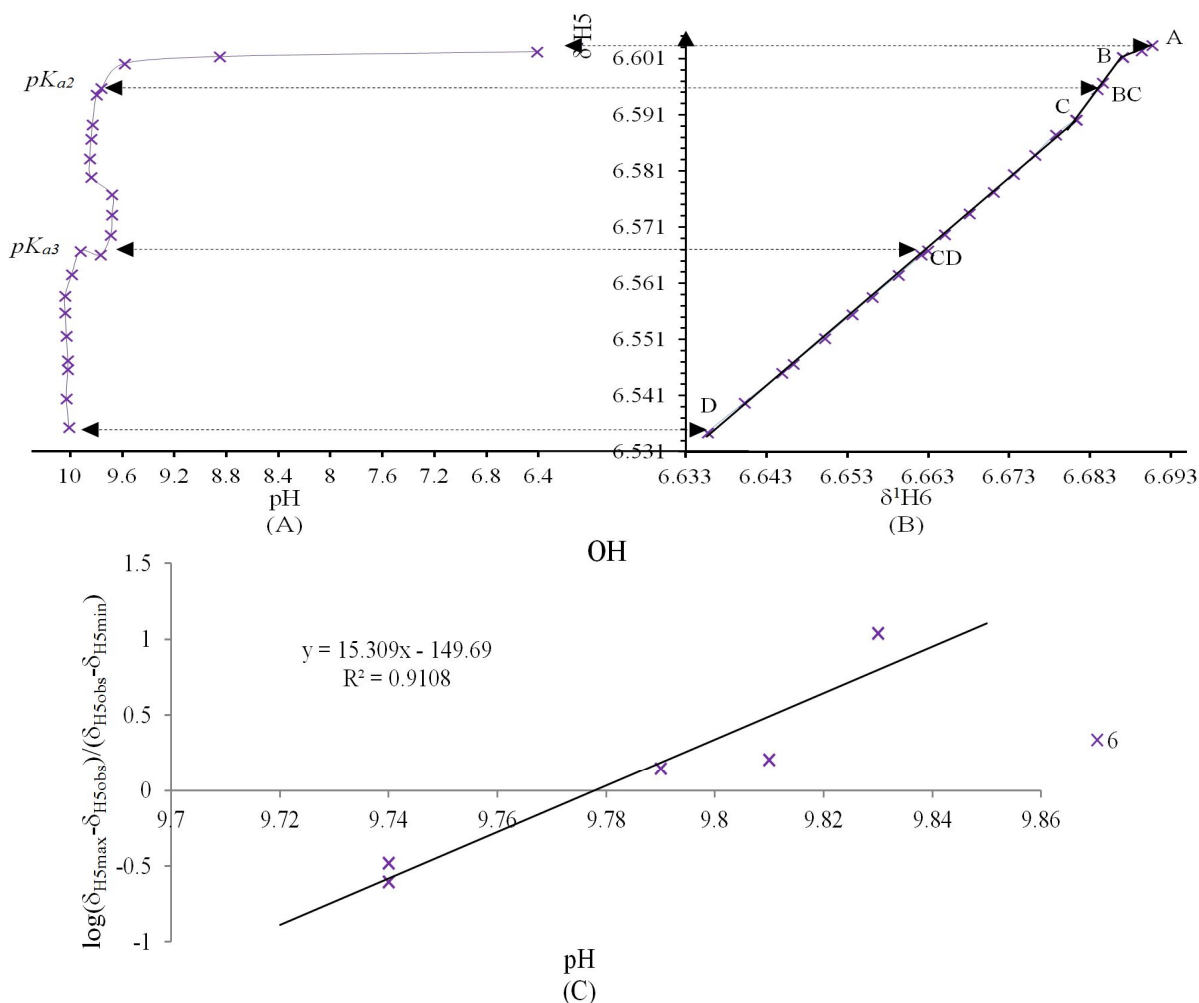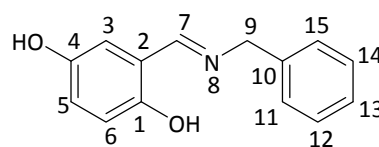
3.5. Data Analysis

The calculations were performed on a Microsoft Excel worksheet. The data analysis of the semilogarithmic Henderson-Hasselbalch (Equation (3)) was applied to data that have adapted to this analysis method, using a dependent variable $\log[(\delta_{Hmax} - \delta_{Hobs})/(\delta_{Hobs} - \delta_{Hmin})]$; H9 for compounds **1**–**5** and H5 for compound **6**) (HX = H5 or H9) and *pH* as an independent variable for titration curves to find the *pKa* values.

Data analysis for the δ-diagram by both Perrin and Polster-Lachmann analysis used H6 and H9 proton chemical shifts for the analysis in δ-diagram, since they are the proton chemical shifts adjacent to NHO intramolecular hydrogen bond and the most affected by deprotonation. Thus in the Perrin Analysis Equation (5) can be written as follows (Equation (7)):

$$\left(\delta_{H9} - \delta_{H9^\circ}\right)\left(\delta_{H6^e} - \delta_{H6}\right) = \Delta K_{NHO}\left(\delta_{H6} - \delta_{H6^\circ}\right)\left(\delta_{H9^e} - \delta_{H9}\right) \tag{7}$$

where δ_{H9° and δ_{H6° are the chemical shifts from the species at the beginning of the titration, δ_{H9} and δ_{H6} the chemical shifts observed in the course of the titration, δ_{H9}^e and δ_{H6}^e are the chemical shifts from species at the end of the titration. Finally in the Polster-Lachmann analysis, the ratio of distances to calculate the ΔK_{NHO} value is established by the graphic method described by the Gibbs triangle [62,68].

4. Conclusions

The study of compounds **1**–**6** by NMR titration in methanol solution, confirmed the predominant tautomeric forms in solution, noting that the NHO prototropic equilibrium is dependent of the substituent and the solvent. The *pKa* values obtained using the Henderson-Hasselbalch analysis showed that all compounds are weak acids. The strength and lability of the NHO intramolecular hydrogen bond are consequently affected by the mesomeric and inductive effects exerted by the substituents. The values of the K_{NHO} equilibrium constant indicate that the equilibrium is slightly shifted to the nitrogen atom when the substituent in the phenyl ring exerts a strong electronic effect, either ED or EW (R = NO_2, Cl, OMe and OH), and to the oxygen atom when Br or H in CD_3OD solutions. Nevertheless the ΔK_{NHO} values close to the unit, highlight that the proton is in the middle of both basic sites ($O^-\cdots H\cdots N^+$), in contrast to what is found in DMSO-d_6 solutions, where NMR data is in agreement with the neutral $N\cdots H–O$ tautomer for most of the compounds except for the nitro derivative which is in the zwitterion $^+N–H\cdots O$ form. Finally, we have demonstrated the simplicity, accuracy and versatility of both the Perrin and Polster-Lachmann analysis applied to the study of intramolecular hydrogen bonds.

Conflicts of Interest

The authors declare no conflict of interest.

References

1. Hodnett, E.M.; Mooney, P.D. Antitumor activities of some Schiff bases. *J. Med. Chem.* **1970**, *13*, 786.
2. Hodnett, E.M.; Dunn, W.J. Cobalt derivatives of Schiff bases of aliphatic amines as antitumor agents. *J. Med. Chem.* **1972**, *15*, 339.
3. Huang, S.C. New Schiff Bases of Aminohydroxyguanidine as Inhibitors of Tumor Cells and QSAR Analysis, M.S. Thesis, University of the Southern California, Los Angeles, CA, USA, 2001.
4. Ren, S. Design, Synthesis, Biological Testing and QSAR Analysis of new Schiff bases of N-Hydroxysemicarbazide as Inhibitors of Tumor Cells, Ph.D. Thesis, University of Southern California, Los Angeles, CA, USA, 2001.
5. Gacche, R.N.; Gond, D.S.; Dhole, N.A.; Dawane, B.S. Coumarin Schiff-bases: As antioxidant and possibly anti-inflammatory agents. *J. Enzym. Inhib. Med. Chem.* **2006**, *21*, 157–161.
6. Krause, M.; Rouleau, A.; Stark, H.; Luger, P.; Lipp, R.; Garbarg, M.; Schwartz, J.-C.; Schunack, W. Synthesis, X-ray crystallography, and pharmacokinetics of novel azomethine prodrugs of (r)-α-methylhistamine: Highly potent and selective histamine h3 receptor agonists. *J. Med. Chem.* **1995**, *38*, 4070–4079.
7. Kaplan, J.P.; Raizon, B.M.; Desarmenien, M.; Feltz, P.; Headley, P.M.; Worms, P.; Lloyd, K.G.; Bartholini, G. New anticonvulsants: Schiff bases of γ-aminobutyric acid and γ-aminobutyramide. *J. Med. Chem.* **1980**, *23*, 702–704.
8. Koneru, P.B.; Lien, E.J.; Avramis, V.I. Synthesis and testing of new antileukemic Schiff bases of N-hydroxy-N'-aminoguanidine against CCRF-CEM/0 human leukemia cells *in vitro* and synergism studies with cytarabine (Ara-C). *Pharm. Res.* **1993**, *10*, 515–520.
9. Gangani, B.J.; Parsania, P.H. Microwave-irradiated and classical syntheses of symmetric double Schiff bases of 1,1'-bis(4-aminophenyl)cyclohexane and their physicochemical characterization. *Spectrosc. Lett.* **2007**, *40*, 97–112.
10. Parekh, J.; Inamdhar, P.; Nair, R.; Baluja, S.; Chanda, S. Synthesis and antibacterial activity of some Schiff bases derived from 4-aminobenzoic acid. *J. Serb. Chem. Soc.* **2005**, *70*, 1155–1161.
11. Shi, L.; Fang, R.; Xue, J.; Xiao, Z.; Tan, S.; Zhu, H. Synthesis, characterization, and antibacterial and cytotoxic study of metal complexes with Schiff base ligands. *Aust. J. Chem.* **2008**, *61*, 288–296.
12. Shi, L.; Ge, H.M.; Tan, S.H.; Li, H.Q.; Song, Y.C.; Zhu, H.L.; Tan, R.X. Synthesis and antimicrobial activities of Schiff bases derived from 5-chloro-salicylaldehyde. *Eur. J. Med. Chem.* **2007**, *42*, 558–564.
13. Venugopala, K.N.; Jayashree, B.S. Microwave-induced synthesis of Schiff bases of aminothiazolyl bromocoumarins as antibacterials. *Indian J. Pharm. Sci.* **2008**, *70*, 88–91.
14. Zheng, B.; Brett, S.J.; Tite, J.P.; Lifely, M.R.; Brodie, T.A.; Rhodes, J. Galactose oxidation in the design of immunogenic vaccines. *Science* **1992**, *256*, 1560–1563.
15. Vazzana, I.; Terranova, E.; Mattioli, F.; Sparatore, F. Aromatic Schiff bases and 2,3-disubstituted-1,3-thiazolidin-4-one derivatives as antiinflammatory agents. *Arkivoc* **2004**, 364–374.
16. Sharif, S.; Powell, D.R.; Schagen, D.; Steiner, T.; Toney, M.D.; Fogle, E.; Limbach, H.H. X-ray crystallographic structures of enamine and amine Schiff bases of pyridoxal and its 1:1

hydrogen-bonded complexes with benzoic acid derivatives: Evidence for coupled inter- and intramolecular proton transfer. *Acta Crystallogr.* **2006**, *B62*, 480–487.

17. Golubev, N.S.; Smirnov, S.N.; Tolstoy, P.M.; Sharif, S.; Toney, M.D.; Denisov, G.S.; Limbach, H.H. Observation by NMR of the tautomerism of an intramolecular OHOHN-charge relay chain in a model Schiff base. *J. Mol. Struct.* **2007**, 319–327.

18. Sharif, S.; Denisov, G.S.; Toney, M.D.; Limbach, H.H. NMR studies of coupled low- and high-barrier hydrogen bonds in pyridoxal-5'-phosphate model systems in polar solution. *J. Am. Chem. Soc.* **2007**, *129*, 6313–6327.

19. Sharif, S.; Huot, M.C.; Tolstoy, P.M.; Toney, M.D.; Jonsson, K.H.M.; Limbach, H.H. [15]N nuclear magnetic resonance studies of acid-base properties of pyridoxal-5'-phosphate aldimines in aqueous solution. *J. Phys. Chem. B* **2007**, *111*, 3869–3876.

20. Lin, Y.L.; Gao, J. Internal proton transfer in the external pyridoxal 5'-phosphate Schiff base in dopa decarboxylase. *Biochemistry* **2010**, *49*, 84–94.

21. Day, J.H. Thermochromism. *Chem. Rev.* **1962**, *63*, 65–80.

22. Minkin, V.I. Photo-, Thermo-, Solvato-, and Electrochromic spiroheterocyclic compounds. *Chem. Rev.* **2004**, *104*, 2751–2776.

23. Hoshino, N.; Inabe, T.; Mitani, T.; Maruyama, Y. Structure and optical properties of a thermochromic Schiff base. Thermally induced intramolecular proton transfer in the *N,N'*-bis(salicylidene)-*p*-phenylenediamine crystals. *Bull. Chem. Soc. Jpn.* **1988**, *61*, 4207–4214.

24. Takeda, S.; Chihara, H.; Inabe, T.; Mitani, T.; Maruyama, Y. NMR study of proton dynamics in the NHO hydrogen in the thermochromic crystals of *N*-salicylideneanilines. *Chem. Phys. Lett.* **1992**, *189*, 13–17.

25. Lambi, E.; Gegiou, D.; Hadjoudis, E. Thermochromism and photochromism of *N*-salicylidene-benzylamines and *N*-salicylidene-2-aminomethylpyridine. *J. Photochem. Photobiol. A Chem.* **1995**, *86*, 241–246.

26. Hadjoudis, E.; Rontoyianni, A.; Ambroziak, K.; Dziembowska, T.; Mavridis, I.M. Photochromism and thermochromism of solid *trans-N.,N'*-bis-(salicylidene)-1,2-cyclohexane-diamines and *trans-N,N'*-bis-(2-hydroxynaphylidene)-1,2-cyclohexanediamine. *J. Photochem. Photobiol. A Chem.* **2004**, *162*, 521–530.

27. Amimoto, K.; Kawato, T. Photochromism of organic compounds in the crystal state. *J. Photochem. Photobiol. C* **2005**, *6*, 207–226.

28. Akitsu, T.; Einaga, Y. A chiral photochromic Schiff base: (*R*)-4-Bromo-2-[(1-phenylethyl)-iminomethyl]phenol. *Acta Crystallogr.* **2006**, *E62*, o4315–o4317.

29. Bolz, I.; May, C.; Spange, S. Solvatochromic properties of Schiff bases derived from 5-amino-barbituric acid: Chromophores with hydrogen bonding patterns as components for coupled structures. *New J. Chem.* **2007**, *31*, 1568–1571.

30. Gegiou, D.; Lambi, E.; Hadjoudis, E. Solvatochromism in N-(2-Hydroxybenzylidene)aniline, *N*-(2-Hydroxybenzylidene)benzylamine, and *N*-(2-Hydroxybenzylidene)-2-phenylethylamine. *J. Phys. Chem.* **1996**, *100*, 17762–17765.

31. Raczynska, E.D.; Kosinska, W.; Osmiałowski, B.; Gawinecki, R. Tautomeric equilibria in relation to pi-electron delocalization. *Chem. Rev.* **2005**, *105*, 3561–3612.

32. Schilf, W. Intramolecular hydrogen bond investigations in some Schiff bases using C-C and N-C coupling constants. *J. Mol. Struct.* **2004**, *689*, 245–249.

33. Schilf, W.; Kamienski, B.; Szady-Chelmieniecka, A.; Grech, E.; Makal, A.; Wozniak, K. NMR and X-ray studies of 2,6-bis(alkylimino)phenol Schiff bases. *J. Mol. Struct.* **2007**, 94–101.

34. Schilf, W.; Cmoch, P.; Szady-Chelmieniecka, A.; Grech, E. Deprotonation of hydrogen bonded Schiff bases by three strong nitrogen bases. *J. Mol. Struct.* **2009**, *921*, 34–37.

35. Claramunt, R.M.; López, C.; Santa María, M.D.; Sanz, D.; Elguero, J. The use of NMR spectroscopy to study tautomerism. *Prog. Nucl. Magn. Reson. Spectrosc.* **2006**, *49*, 169–206.

36. Dziembowska, T.; Ambroziak, K.; Majerz, I. Analysis of the vibrational spectra of *trans-N,N'*-bis-salicylidene-1',2'-cyclohexanediamine tautomers. *J. Mol. Struct.* **2005**, *738*, 15–24.

37. Filarowski, A. Intramolecular hydrogen bonding in *o*-hydroxyaryl Schiff bases. *J. Phys. Org. Chem.* **2005**, *18*, 686–698.

38. Filarowski, A.; Koll, A.; Rospenk, M.; Krol-Starzomska, I.; Hansen, P.E. Tautomerism of sterically hindered Schiff bases. Deuterium isotope effects on ^{13}C chemical shifts. *J. Phys. Chem. A* **2005**, *109*, 4464–4473.

39. Raczynska, E.D.; Krygowski, T.M.; Zachara, J.E.; Osmiałowski, B.; Gawinecki, R. Tautomeric equilibria, H-bonding and π-electron delocalization in *o*-nitrosophenol. A B3LYP/ 6–311+G(2df,2p) study. *J. Phys. Org. Chem.* **2005**, *18*, 892–897.

40. Osmiałowski, B.; Raczynska, E.D.; Krygowski, T.M. Tautomeric equilibria and pi electron delocalization for some monohydroxyarenes-quantum chemical studies. *J. Org. Chem.* **2006**, *71*, 3727–3736.

41. Filarowski, A.; Kochel, A.; Kluba, M.; Kamounah, F.S. Structural and aromatic aspects of tautomeric equilibrium in hydroxyaryl Schiff bases. *J. Phys. Org. Chem.* **2008**, *21*, 939–944.

42. Kluba, M.; Lipkowski, P.; Filarowski, A. Theoretical investigation of tautomeric equilibrium in *ortho*-hydroxy phenyl Schiff bases. *Chem. Phys. Lett.* **2008**, *463*, 426–430.

43. Salman, S.R.; Lindon, J.C.; Farrant, R.D.; Carpenter, T.A. Tautomerism in 2-hydroxy-1-naphthaldehyde Schiff bases in solution and the solid state investigated using ^{13}C-NMR spectroscopy. *Magn. Reson. Chem.* **1993**, *31*, 991–994.

44. Salman, S.R.; Kamounah, F.S. Tautomerism in 1-hydroxy-2-naphthaldehyde Schiff bases: Calculation of tautomeric isomers using carbon-13 NMR. *Spectrosc.-Int. J.* **2003**, *17*, 747–752.

45. Santos-Contreras, R.J.; Ramos-Organillo, A.; Garcia-Baez, E.V.; Padilla-Martinez, I.I.; Martinez-Martinez, F.J. The zwitterion of 4-nitro-2-{(E)-[2-(piperidin-1-yl)ethyl]iminomethyl}phenol. *Acta Crystallogr.* **2009**, *C65*, o8–o10.

46. Pyta, K.; Przybylski, P.; Schilf, W.; Kolodziej, B.; Szady-Chelmieniecka, A.; Grech, E.; Brzezinski, B. Spectroscopic and theoretical studies of the protonation of *N*-(5-nitrosalicylidene)-ethylamine. *J. Mol. Struct.* **2010**, *967*, 140–146.

47. Filarowski, A.; Glowiaka, T.; Koll, A. Strengthening of the intramolecular O¨H¨N hydrogen bonds in Schiff bases as a result of steric repulsion. *J. Mol. Struct.* **1999**, *484*, 75–89.

48. Przybylski, P.; Schroeder, G.; Brzezinski, B.; Bartl, F. ^{1}H-NMR, FT-IR and MS studies and PM5 semiempirical calculations of complexes between the Schiff base of gossypol with 2-(aminomethyl)-15-crown-5 and Ca^{2+}, Pb^{2+} and Ba^{2+} cations. *J. Phys. Org. Chem.* **2003**, *16*, 289–297.

49. Dziembowska, T.; Rozwadowski, Z.; Filarowski, A.; Hansen, P.E. NMR study of proton transfer equilibrium in Schiff bases derived from 2-hydroxy-1-naphthaldehyde and 1-hydroxy-2-acetonaphthone. Deuterium isotope effects on ^{13}C and ^{15}N chemical shifts. *Magn. Reson. Chem.* **2001**, *39*, S67–S80.

50. Sharif, S.; Denisov, G.S.; Toney, M.D.; Limbach, H.H. NMR studies of solvent-assisted proton transfer in a biologically relevant Schiff base: Toward a distinction of geometric and equilibrium H-bond isotope effects. *J. Am. Chem. Soc.* **2006**, *128*, 3375–3387.

51. Rozwadowski, Z.; Nowak-Wydra, B. Chiral recognition of Schiff bases by ^{15}N-NMR spectroscopy in the presence of a dirhodium complex. Deuterium isotope effect on ^{15}N chemical shift of the optically active Schiff bases and their dirhodium tetracarboxylate adducts. *Magn. Reson. Chem.* **2008**, *46*, 974–978.

52. Kamounah, F.S.; Salman, S.R.; Mahmoud, A.A.K. Substitution and solvent effect of some substituted hydroxy schiff bases. *Spectrosc. Lett.* **1998**, *31*, 1557–1567.

53. Irle, S.; Krygowski, T.M.; Niu, J.E.; Schwarz, W.H.E. Substituent effects of -NO and -NO$_2$ groups in aromatic systems. *J. Org. Chem.* **1995**, *60*, 6744–6755.

54. Krygowski, T.M.; Stepien, B.T. Sigma- and pi-electron delocalization: Focus on substituent effects. *Chem. Rev.* **2005**, *105*, 3482–3512.

55. Otto, E.; Stanislav, B. Substituent effects of the alkyl groups: Polarity *vs.* Polarizability. *Eur. J. Org. Chem.* **2007**, *2007*, 2870–2876.

56. Ozeryanskii, V.A.; Pozharskii, A.F.; Schilf, W.; Kamieński, B.; Sawka-Dobrowolska, W.; Sobczyk, L.; Grech, E. Novel polyfunctional tautomeric systems containing salicylideneamino and proton sponge moieties. *Eur. J. Org. Chem.* **2006**, *2006*, 782–790.

57. Gilli, G.; Bellucci, F.; Ferretti, V.; Bertolasi, V. Evidence for resonance-assisted hydrogen bonding from crystal-structure correlations on the enol form of the β-diketone fragment. *J. Am. Chem. Soc.* **1989**, *111*, 1023–1028.

58. Gilli, P.; Bertolasi, V.; Ferretti, V.; Gilli, G. Towards an unified hydrogen-bond theory. *J. Am. Chem. Soc.* **2000**, *122*, 10405–10417.

59. Gilli, P.; Bertolasi, V.; Pretto, L.; Antonov, L.; Gilli, G. Variable-temperature X-ray crystallographic and DFT computational study of the N-H···O/N···H-O tautomeric competition in 1-(Arylazo)-2-naphthols. Outline of a transiton-state hydrogen-bond theory. *J. Am. Chem. Soc.* **2005**, *127*, 4943–4953.

60. Dominiak, P.M.; Grech, E.; Barr, G.; Teat, S.; Mallinson, P.; Wozniak, K. Neutral and ionic hydrogen bonding in Schiff bases. *Chem. Eur. J.* **2003**, *9*, 963–970.

61. Krygowski, T.M.; Wozniak, K.; Anulewicz, R.; Pawlak, D.; Kolodziejski, W.; Grech, E.; Szady, A. Through-resonance assisted ionic hydrogen bonding in 5-Nitro-N-salicylideneethylamine. *J. Phys. Chem. A* **1997**, *101*, 9399–9404.

62. Polster, J.; Lachmann, H. *Spectrometric Titration: Analysis of Chemical Equilibria*; VCH Verlagsgesellschaft: Weinheim, Germany, 1989; pp. 33–132.

63. Macomber, R.S. An introduction to NMR titration for studying rapid reversible complexation. *J. Chem. Educ.* **1992**, *69*, 375.

64. Breitmaier, E.; Spohn, K.-H. P$_H$-abhängigkeit der ^{13}C-chemischen verschiebungen sechsgliedriger stickstoff-heteroaromaten. *Tetrahedron* **1973**, *29*, 1145.

65. Breitmaier, E.; Voelter, W. *Carbon-13 NMR Spectroscopy: High Resolution Methods and Applications in Organic Chemistry and Biochemistry*, 3rd ed.; VCH Verlagsgesellschaft GbBH: New York, NY, USA, 1990; pp. 107–123.

66. Szakács, Z.; Hägele, G. Accurate determination of low pK values by ^{1}H-NMR titration. *Talanta* **2004**, *62*, 819–825.

67. Berger, S. A ^{13}C magnetic resonance study. *Tetrahedron* **1977**, *33*, 1587–1589.

68. Gobber, F.; Polster, J. Determination of relative pK values of dibasic protolytes by regression analysis of absorbance diagrams. *Anal. Chem.* **1976**, *48*, 1546–1550.

69. Perrin, C.L.; Thoburn, J.D. Evidence for a double-minimum potential for intramolecular hydrogen bonds of aqueous hydrogen maleate and hydrogen phthalate anions. *J. Am. Chem. Soc.* **1989**, *111*, 8010–8012.

70. Miles, A.F.; Perrin, C.L.; Sinnott, M.L. Absence of reverse anomeric effect: Conformational analysis of glucosylimidazolium and glucosylimidazole. *J. Am. Chem. Soc.* **1994**, *116*, 8398–8399.

71. Perrin, C.L.; Fabian, M.A.; Armstrong, K.B. Solvation effect on steric bulk of ionic substituents: Imidazolium *vs.* imidazole. *J. Org. Chem.* **1994**, *59*, 5246–5253.

72. Perrin, C.L.; Fabian, M.A. Multicomponent NMR titration for simultaneous measurement of relative pK$_a$s. *Anal. Chem.* **1996**, *68*, 2127–2134.

73. Makal, A.; Schilf, W.; Kamienski, B.; Szady-Chelmieniecka, A.; Grech, E.; Wozniak, K. Hydrogen bonding in Schiff bases-NMR, structural and experimental charge density studies. *Dalton Trans.* **2011**, *40*, 421–430.

Sample Availability: Samples of the compounds **1**–**6** are available from the authors.